Carbohydrate Research, 217 (1991) 29–42
Elsevier Science Publishers B.V., Amsterdam

Conformational analysis of 1-kestose by molecular mechanics and by n.m.r. spectroscopy*

Andrew L. Waterhouse†, Thomas M. Calub,
Department of Chemistry, Tulane University, New Orleans, Louisiana 70118 (U.S.A.)
and Alfred D. French
Southern Regional Research Center, United States Department of Agriculture, P.O. Box 19687, New Orleans, Louisiana 70179 (U.S.A.)

(Received July 16th, 1990; accepted with revisions December 17th, 1990)

ABSTRACT

Models of the trisaccharide, 1-kestose [β-D-fructofuranosyl-(2→1)-β-D-fructofuranosyl-(2↔1)-α-D-glucopyranoside], were analyzed with the molecular mechanics computer program MM2(87) to ascertain their inter-ring torsion angles, primary alcohol side-group orientations, and ring puckering. The most striking result was that the modeling predicted and n.m.r. spectroscopy corroborated that the central fructofuranose ring takes a different form from that previously observed in the crystal. No other studies of fructofuranoses have observed that crystallographic form, thus suggesting that the 18 hydrogen bonds created upon crystallization of 1-kestose support the ring deformation. Because this trisaccharide is too complex for a complete study of conformation space, only structures having inter-ring conformations that were at energetic valleys in previous studies of the constituent disaccharides were analyzed. The model of 1-kestose with lowest energy had inter-ring torsion angles that did not correspond to the global minima of the model disaccharides, although they were generally close to the linkage conformations observed in the crystal structure, differing by an average of 19°.

INTRODUCTION

1-Kestose (1) was first observed during the action of yeast invertase preparations on concentrated sucrose solutions[1]. It occurs naturally in honey[2] and in numerous plants[3]. Concentrations of oligomers and polymers of fructans have been correlated with cold-stress response in plants[4], and there are a number of potential commercial applications[5]. As shown in Fig. 1, 1 corresponds to sucrose with an additional fructose residue and thus is the trisaccharide prototype for the inulin family of oligomers and polymers. Two other kestoses are also known, with their second fructosyl residues linked at the other two primary alcohol groups of the sucrose moiety.

The present study continues our efforts to learn the likely shapes of oligomers and polymers of fructofuranose. In this context, interesting conformational aspects of 1 include the torsion angles for the bonds linking the monosaccharide residues, the orientations of the primary alcohol groups, and the puckering of the sugar rings. The

* Paper no. 3 of a series, Conformational Analysis of Fructans.
† Author to whom correspondence should be addressed. Current address: Department of Viticulture and Enology, University of California, Davis, CA 95616 (U.S.A.).

0008-6215/91/$03.50

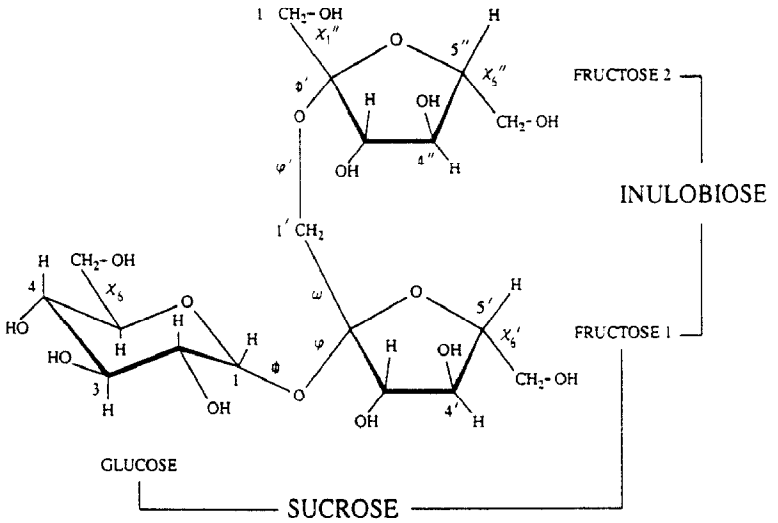

Fig. 1. 1-Kestose with torsion angles labeled: φ is defined by H-1–C-1–O–C-2′, ψ is defined by C-1–O–C-2′–O-5′, φ' is defined by C-1″–C-2″–O–C-1′, ψ' is defined by C-2″–O–C-1′–C-2′, and ω is defined by O–C-1′–C-2′–O-2′. The χ-6 angles are defined using the hydroxymethyl oxygens and the endocyclic oxygen. The χ-1″ angle is defined by O-1″–C-1″–C-2″–O (linkage O).

present work draws upon results from two previous studies of the sucrose[6] and inulobiose[7] disaccharide for likely ring forms, for values of the inter-ring torsion angles, and for orientations of the rotatable side groups to create initial structures which would lead to the most probable forms of **1**. More than four-hundred such forms were optimized and their energies compared.

In order to obtain experimental confirmation of our proposed conformation, proton and carbon n.m.r. studies were conducted on **1** in aqueous (D_2O) solution. Conformational information was extracted from vicinal coupling constants, some of which were presented in an earlier paper[8]. An X-ray crystallographic structure of **1** has been determined by Jeffrey and Park, and this structure is compared with the model and the solution data[9]. This crystallographic structure is unusual in that the central fructose ring has a unique form and the hydroxymethyl side-group of glucose is disordered and includes the unusual *tg* form.

EXPERIMENTAL

Computational details and n.m.r. methods. — All molecular modeling analyses were carried out using the molecular modeling program MM2(87)[10] ported to an IBM 3081/3090 series mainframe computer. The program was modified to drive as many as eight torsion angles simultaneously. Also, an additional type of driver was provided to start each minimization from the initial internal residue conformation rather than from geometries from the preceding result[11]. The default dielectric constant and optimization termination criteria were used.

The force-field used by MM2(87) is one of the better ones available for carbohydrates. Parameters were incorporated for carbohydrates in the 1985 version[12] of the program to compensate for the varied bond length associated with anomeric centers and are retained in this version. In addition, the treatment of H-bonding was refined in the 1987 version. However, because the the calculations are carried out on isolated or gas phase molecules, there are, as expected, some differences with solution data. The internal dielectric constant correction factor has little effect and was not used.

The molecular model of 1-kestose used in the MM2(87) calculations was created by fusing a previously optimized $^4C_1$ glucose and the structure of inulobiose found to have the lowest energy in our pevious molecular modeling study[7]. The hydroxymethyl side-groups were first oriented in the preferred positions as previously determined[6,7,13].

An initial search (run A) of the conformational energy of **1** was carried out by setting the torsion angles φ, ψ, φ', and ω (see Fig. 1) at $-60°$ and driving them in 120° increments, generating all the staggered combinations of these four linkage angles. In the second survey (run B), the torsion angle φ was set initially at 0° and rotated at steps of 120°. The three other torsion angles were rotated in the same manner as in A, starting at $-60°$. The next search (run C) was carried out by driving the torsion angle φ from $-30°$ to $+30°$ in 30°-steps and the torsion angles ψ, φ', and ω in the same manner as before. In all the searches made, ψ' was set at 165° and allowed to relax to its local minimum.

The local minima from all the three runs were then extracted and re-optimized without any restrictions, and their fully relaxed conformations were determined and compared. While all structures within 10 kcal·mol^{-1} above the lowest energy found in each run were included for re-optimization, Table I shows only those structures having fully relaxed energies within 5 kcal·mol^{-1} above the B1 minimum.

The nature of the energy valley near the synperiplanar region of φ was studied by driving φ of B1 in 2° increments from $-60°$ to $+30°$. Partial results are plotted in Fig. 2 (Run D).

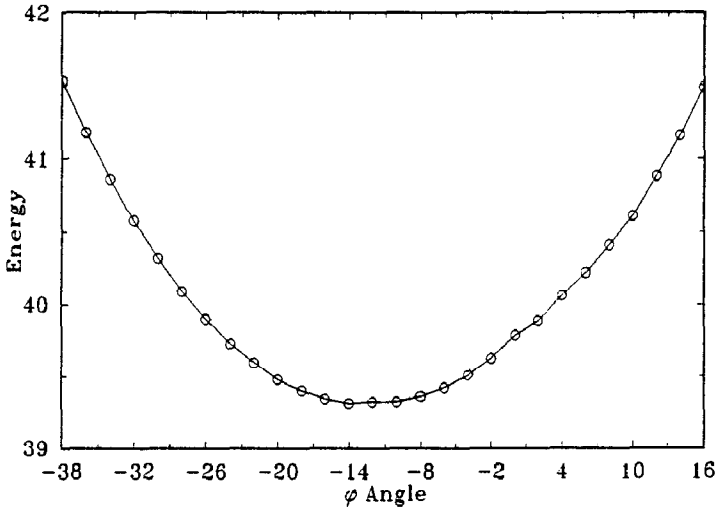

Fig. 2. A plot of steric energy *vs.* the torsion angle of φ, with φ driven at 2° increments starting with the B1 structure (run D).

TABLE I

Torsion angles and energies of all the local minima from runs A to C[a]

	φ	ψ	φ'	ψ'	ω	χ_6[b]	χ_6'	χ_6''	χ_1''	*Energy*
SS	D	D	D	165.67	D	−65.38	−60.84	−58.67	58.20	
XR1	−35.33	−65.69	88.84	−162.34	42.54	−74.06	64.54	64.22	179.19	72.18
XR2	−32.31	−65.65	88.71	162.12	42.52	−53.37	54.76	53.61	−179.65	55.18
XR3	−13.56	−55.31	53.40	173.00	55.66	−57.29	52.85	53.43	172.24	43.07
A1	−60.00	−60.00	−60.00	168.86	60.00	−64.32	−70.30	−58.77	90.70	48.23
	−54.78	−83.83	−44.37	175.67	57.95	−63.63	−66.28	−61.42	83.83	43.85
A2	−60.00	−60.00	60.00	179.86	60.00	−64.67	−67.98	−55.17	57.57	48.78
	−30.07	−69.27	59.85	−176.23	48.04	−64.96	−66.99	−57.89	59.24	43.49
A3	−60.00	180.00	60.00	168.56	180.00	−62.94	−58.86	−64.08	60.59	54.93
	−23.53	−158.75	49.31	159.51	−169.49	−73.01	−54.94	−61.51	62.18	43.32
B1	0.00	−60.00	60.00	169.13	60.00	−61.67	−60.28	−57.92	59.86	45.44
	−12.22	−58.74	51.35	175.73	54.03	−60.76	−55.00	−56.94	51.62	39.33
B2	0.00	−60.00	60.00	166.61	180.00	−61.69	−59.79	−62.21	62.00	45.72
	−8.07	−52.72	51.10	165.88	−174.67	−61.76	−55.59	−62.39	61.99	42.94
B3	0.00	−60.00	60.00	169.36	−60.00	−61.28	−61.90	10.59	59.84	47.98
	−4.47	−53.11	49.14	176.31	−66.87	−61.39	−57.90	21.84	58.48	43.49
B4	0.00	60.00	60.00	167.78	−60.00	−63.45	−62.40	−59.03	60.83	51.74
	8.41	53.02	49.93	176.54	−57.54	−62.38	−51.80	−56.70	60.24	43.82
B5	0.00	−60.00	180.00	170.33	60.00	−62.32	−58.22	−70.57	66.94	54.22
	−10.47	−48.04	−175.85	−173.71	61.54	−61.72	−56.96	−47.45	72.32	43.88
B6	0.00	−60.00	−60.00	168.67	60.00	−62.52	−60.83	−52.82	83.43	54.61
	−13.98	−50.55	−36.17	175.65	61.90	−60.10	−56.53	−60.14	80.82	42.36

C1	−30.00	−60.00	60.00	176.75	60.00	−63.64	−53.38	−53.16	51.35	41.61
	−13.05	−64.02	53.39	176.17	58.02	−62.50	−55.18	−52.78	53.39	39.55
C2	−30.00	−60.00	−60.00	172.87	60.00	−64.17	−52.38	−50.44	90.33	44.87
	−18.84	−53.78	−37.34	164.34	60.17	−61.49	−54.66	−58.81	82.27	41.47
C3	−30.00	−60.00	60.00	170.15	−60.00	−62.52	−54.67	−57.25	55.45	46.54
	−9.72	−55.18	60.49	−168.48	−70.62	−62.08	−56.27	−59.39	54.72	42.16
C4	30.00	60.00	60.00	166.34	180.00	−62.26	−61.21	−62.01	60.27	48.02
	12.58	54.41	51.33	167.74	−173.06	−62.86	−53.86	−61.49	60.82	44.06
C5	0.00	180.00	60.00	173.84	180.00	−64.35	−53.27	−63.39	60.50	49.20
	−20.64	−159.69	47.84	163.54	−171.38	−73.88	−54.82	−61.58	62.12	43.29
C6	30.00	−60.00	180.00	−178.41	−60.00	−62.53	−62.00	−52.45	66.09	49.56
	−16.37	−38.38	171.16	179.01	−56.50	−60.43	−58.94	−52.38	62.69	42.14
C7	30.00	−60.00	60.00	167.23	180.00	−62.31	−57.62	−61.04	60.90	51.94
	−7.54	−50.98	49.95	167.17	−178.17	−61.71	−56.24	−62.13	61.95	42.83

[a] The second entry in each column indicates the torsion angles and energies of the fully relaxed forms. "SS" represents the starting conformation of **1** used in runs A to C, "XR1" represents the crystallographic conformation of **1** with the hydrogens optimized, "XR2" represents the crystallographic conformation relaxed except for the torsion angles, "XR3" represents the fully optimized form of the crystallographic structure, and "D" indicates the torsion angles that were driven. [b] +60° form ≡ *gt*, −60° form ≡ *gg*, 180° form ≡ *tg*.

TABLE II

Torsion angles from local minima of run E[a]

	φ	Ψ	ψ'	Ψ''	ω	χ_6	χ_6'	χ_6''	χ_1''	*Energy*
SS[b]	−12.22	−58.74	51.35	175.73	54.03	D	D	D	D	
E1	−11.88	−58.96	48.56	177.18	55.25	−60.00	−60.00	−60.00	60.00	39.74
	−12.08	−59.06	50.65	176.17	53.94	−60.89	−55.15	−57.84	51.97	39.28
E2	−12.63	−59.43	47.58	177.87	54.67	60.00	−60.00	−60.00	60.00	40.01
	−14.49	−59.89	51.82	176.64	51.87	58.32	−69.85	−56.64	51.10	39.15[c]
E3	−13.08	−56.00	49.63	176.76	54.95	−60.00	180.00	−60.00	60.00	42.92
	−17.23	−56.44	51.57	178.35	50.93	−63.05	176.31	−57.83	51.42	41.23
E4	−12.05	−59.00	51.34	175.74	53.71	−60.00	−60.00	60.00	60.00	41.07
	−12.57	−59.96	55.01	174.10	52.17	−61.29	−54.63	64.73	50.04	40.28
E5	−13.45	−59.76	51.40	176.10	52.67	60.00	−60.00	60.00	60.00	41.15
	−15.47	−61.60	56.10	175.13	50.79	58.78	−68.53	64.78	49.52	39.97
E6	−11.99	−58.74	50.09	176.90	53.85	−60.00	−60.00	180.00	60.00	42.00
	−12.05	−59.26	54.50	173.54	52.08	−61.05	−54.86	176.55	50.52	39.39

[a] For details, see Table I. [b] Starting structure, optimized local minimim B1. "D" indicates the torsion angles that were driven. [c] Global Minimum.

A search for likely orientations of the hydroxymethyl groups was also carried out (run E). Again, the B1 conformation was used as the starting point for the calculations. The search drove all the torsion angles defining the hydroxymethyl groups at 120° increments, starting at −60°. The structures having energies up to 3 kcal·mol^{-1} over the lowest minimum of run E were then extracted and re-optimized (Table II). In Table II, only structures having re-optimized energies within 2 kcal·mol^{-1} of the lowest energy were included. Runs A, B, C, and E each optimized the conformations and energy of 81 starting structures, each taking approximately 12 h of IBM 3081 KX time.

The vacuum-phase energy of the crystallographically determined conformation[9] was compared with energies of the models in three steps. In the first (XR1), the starting model used the crystallographic coordinates and only the hydrogen atoms were allowed to move during minimization, preserving the exact conformation of the rings and interresidue linkages. Relaxation of the hydrogen atoms is needed because these are poorly located by X-ray diffraction work. In the second calculation, the five linkage torsion angles were held at the crystallographically determined angles, but all other parameters were allowed to relax to their local minimum to give XR2. In the third (XR3), all atoms were allowed to move, presumably relieving any intra-molecular strain from intermolecular interactions (Tables I and III).

The Cremer–Pople puckering parameters of the sugar rings were assessed with a program written by Larry Madsen and are listed in Table III and Fig. 3.

Nuclear magnetic resonance spectroscopy experiments were carried out using a Bruker AF 200 narrow-bore spectrometer with a broad-band probe operating at 200.13 MHz for ^{1}H and 50.32 MHz for ^{13}C and a Bruker AM 400 operating at 400.13 MHz for ^{1}H 100.61 MHz for ^{13}C. The heteronuclear-selective *J*-resolved experiment[8] was carried out using the Bruker AF 200. H-1 of the glucose residue was irradiated using a Gaussian pulse, and all the C nuclei coupled to the irradiated proton through three bonds were

TABLE III

Puckering parameters of selected minima, and the crystal structure of 1[a]

	Fruc 1	*Fruc 2*	*Glucose*			*Energy*
	φ_2	φ_2	Q	θ	φ	
SS	266.95	263.10	0.5600	2.82	222.28	
XR1	100.60	254.40	0.5713	8.62	288.40	72.18
XR2	93.17	268.31	0.5517	4.44	152.27	55.18
XR3	119.88	269.67	0.5635	6.97	203.41	43.07
B1	266.32	268.58	0.5476	9.51	226.01	45.44
	277.47	272.68	0.5559	6.62	195.22	39.33
E2	286.42	270.89	0.5605	5.35	191.62	40.01
	286.93	271.88	0.5618	5.69	186.66	39.15[b]

[a] "SS", "XR1", "XR2", and "XR3", represent the puckering parameters of the starting structure, the crystal structure of 1 (with the Hs optimized), the optimized structure with the linkage torsion angles held rigidly, and the fully optimized crystal structure of 1, respectively. [b] Global Minimum

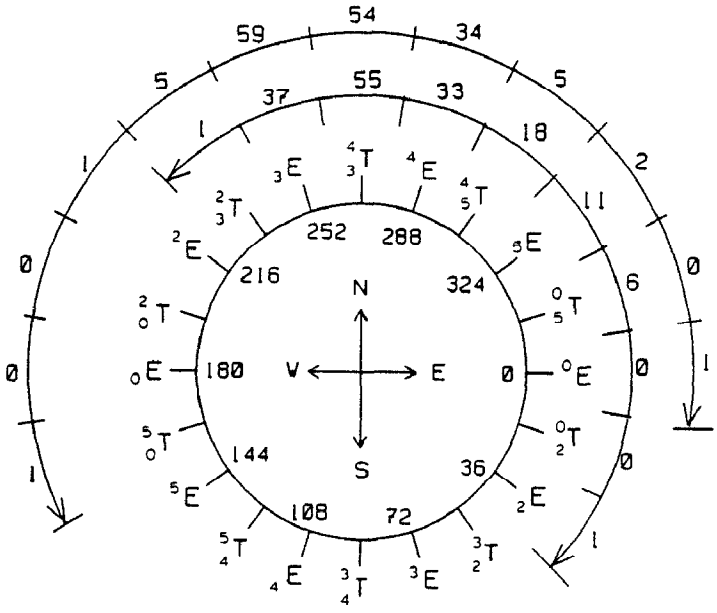

Fig. 3. Conformations, φ_2, shown on a Cremer–Pople standard wheel, for all the structures observed in runs A and B; Fructose 1 (inside) and Fructose 2 (outside).

observed. Each spectrum was obtained by using 80 experiments of 200 scans each and collecting 2000 data points. Data collection took about 3.5 h. The $^3J_{H-H}$ coupling between the H-3s, H-4s, and H-5s of the two fructose residues were determined at 400.13 MHz using a homonuclear (H–H) *J*-resolved experiment. This spectrum was obtained by using 64 experiments of 16 scans each and collecting 1000 data points. The data collection took about 1 h.

RESULTS AND DISCUSSION

Molecular modeling and n.m.r. analysis. — The goal in conformational analysis is to determine the molecular steric energy at all possible combinations of the molecule's geometric variables. This is rarely possible except with the simplest systems. For more complex systems one must choose which variables will provide useful information. In this modeling analysis on 1, eight variables were directly analyzed: four linkage and four side-group torsion angles.

With eight dimensions in this analysis, it is difficult to present the data graphically, and, although it would be possible to present two dimensions at a time with contour plots, this presentation does not facilitate an understanding of the data. Instead, the results from each variable or sets of similar variables were extracted and summarized in the following section.

A conformational energy search was carried out using multiple dihedral angle drivers at 120° increments. Since each of the angles is held rigidly during the mini-

mization, and these angles may not be very close to the optimum, the energies found in this type of survey may be quite far from the minima of the relaxed molecule with the same staggered (or other) forms. Consequently, we found it important to re-optimize without restrictions each resulting structure that was close to the minimum of the driver run. The energy criteria for choosing structures for this fully relaxed analysis depended on the range of energies of each study.

Linkage conformations. — A. The φ angle. The φ angle of the sucrosyl linkage was started at all staggered and eclipsed positions, because in sucrose energy minima have been found when $\varphi = 0°$ and $-20°$ (ref. 6).

Table I shows that two other structures had energies within approximately 2 kcal of the minimum, B1. Inspection reveals that C1 is nearly identical to B1, and these two models would converge to the same structure if the minimizations were continued with a smaller termination energy. The other low-energy structure, C2 has the other gauche form for φ′; however, its energy is 2.1 kcal/mole higher than B1, and thus its population will be about 3% of B1. The other minima are even higher in energy, and their populations are even smaller.

To search for any separate minima in φ between 0° and −60°, as was found for sucrose, the B1 structure was used as the starting point for a study of φ, observing the energy at every 2° increment from −60° to +30° (run D). A continuous valley was found, and the results are plotted in Fig. 2. The minimum is at −14°, but substantial populations are predicted that have φ values between −37° and 15°, the points with energies 2 kcal·mol^{-1} higher than the minimum. Fig. 4 shows the position of φ in the global minimum structure.

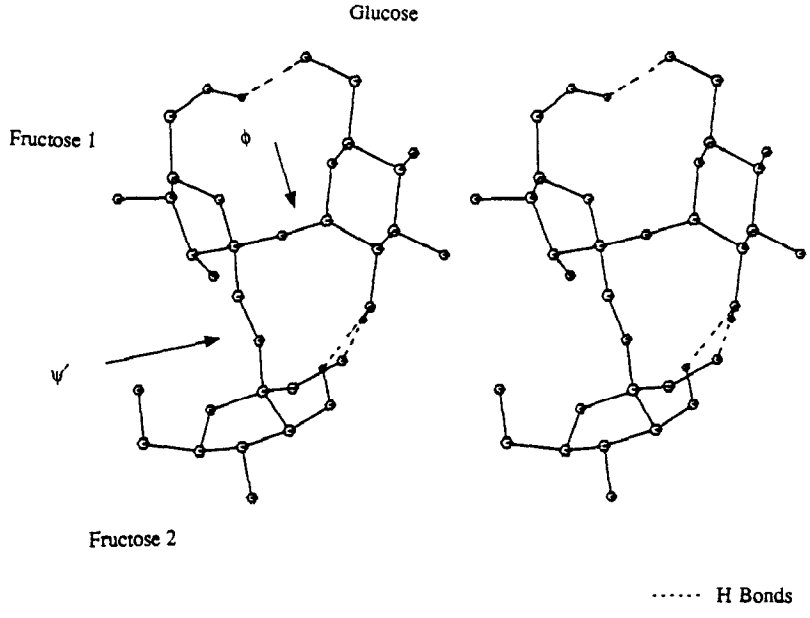

Fig. 4. 1-Kestose with the φ and ψ′ bonds, and H bonds labeled for global minimum (E2).

TABLE IV

Expected coupling constants resulting from the B1 model and the crystallographic conformation XR1, compared with the experimentally observed coupling constants in D_2O for H-3–H-4 pairs on fructose 1 and fructose 2

Atoms	*Torsion angle/calculated coupling constant (Hz)*[16]				*Experimental coupling (Hz)*
	B1	J_{cal}	*XR1*	J_{cal}	J_{obs}
H-3′–H-4′	147°	7.0	84°	0.1	8.0
H-4′–H-5′	−151°	7.6	−92°	0.0	8.5
H-3″–H-4″	147°	7.0	165°	9.3	8.0
H-4″–H-5″	−149°	7.3	−153°	8.0	7.5

Since n.m.r. detects average signals from rapidly interconverting forms of the molecule, all these structures contribute to the observed n.m.r. spectrum of **1**. And, since vicinal coupling is not a linear function of the torsion angle, it must be calculated for each population and then averaged. The $^3J_{C-H}$ within the φ angle, through atoms H-1–C-1–O–C-2′, was calculated using the Eq. *1* determined for H–C–O–C in sugars[14].

$$^3J_{C-H} = 0.5 - 0.6\cos\Theta + 5.7\cos^2\Theta \qquad (1)$$

Calculating this value for each 2° increment and averaging over the population at each point[15], the predicted $^3J_{C-H}$ value obtained from this calculation was 5.2 ± 0.5 Hz. The experimental $^3J_{C-H}$ obtained from the selective *J*-resolved spectrum was 4.3 Hz[8]. If one estimates the φ angle directly from the above theoretical expression, assuming the same staggered form and no flexibility, a coupling constant of 4.3 Hz would yield a torsion angle of −30°.

It is not clear if the discrepancy is primarily due to errors in the above torsion angle expression, or from errors in the models. The above expression was created by analyzing $^3J_{C-H}$ in rigid carbohydrates, and it is possible that the hybridization of the carbons in the models was affected, potentially altering the measured coupling constants. Most of the difference is probably due to the absence of water as solvent in the modeling calculations, which would result in the overemphasis of some intramolecular H-bonding. The discrepancy of 16° may appear small, but the problem merits further study with modeling systems that better account for the effects of solvent.

In the crystal structure[9] of **1**, $\varphi = -35.33°$, but in the relaxed structure (XR3), $\varphi = -13.5°$, surprisingly close to the angle found in B1 considering that the ring puckering in fructose 1 was so different (see below). This result highlights the insensitivity to ring form in this structure where the oligomeric backbone does not include bonds in the monomer rings.

B. ψ, φ', *and* ω. These angles all prefer staggered forms, even though at least one staggered conformation created steric problems. For each torsion angle, steric collision

arises between the two sucrose components when ψ is at $+60°$; thus, $-60°$ appears to be favored. The φ' angle occurs at 60° in most of the low-energy structures, as was observed for inulobiose, although all staggered forms appear in minima. The ω angle is populated with all staggered forms, but unlike inulobiose, the 60° angle is preferred over $-60°$ because when ω is at $-60°$, the glucose ring is too close to the fructose 2 ring.

C. The ψ' angle. Based on results with inulobiose[7], the ψ' angle was started in the antiperiplanar form and allowed to relax during the minimizations. The antiperiplanar conformation was retained in most cases. A few of the structures were found with the anticlinal conformation, but none were found with the synclinal or synperiplanar conformation. In nearly all cases, the final value of ψ' angle was in the range of 150°–180°. Fig. 4 shows the orientation of psi in the global minimum. The crystal structure has a value of $-162°$, but this rotates to 173° on optimization (XR3).

Orientations of the hydroxymethyl groups. — Using structure B1 as the starting point, the four hydroxymethyl groups were rotated through the three staggered forms in series E. Table II shows the final conformations of the six local minima. Structures having energies within 3.5 kcal·mol^{-1} of the lowest energy structure found are included. It was clear that 60° is the preferred angle for χ-1″, the same as found for inulobiose. This same angle has a value of 179.2° in the crystal structure of **1**, due to inter-molecular H-bonding[9].

The energies for both gauche forms for χ-6, (minima at $+58°/gg$ and $-61°/gt$) differed by only 0.13 kcal·mol^{-1} (E1 and E2 respectively), indicating that the two forms would be almost equally populated. In the crystal structure of **1**, this same χ-6 angle was found to be disordered, having two populations, at $-74°/gt$ (66%) and $177°/tg$ (34%). The presence of the *tg* form in the crystal structure is attributed to an intermolecular H-bond. The stability of the *gt* form in E2 is certainly influenced by an intramolecular H-bond which can be achieved in this form between O-6 and O-6′ (Fig. 4).

For χ-6′, two accessible conformations were found, one at $-60°$ and one at 180°, but the $-60°$ form was more stable by nearly 2 kcal·mol^{-1}. On the other hand, χ-6″ had low energy values at all staggered forms. The largest difference separating two staggered conformers was only 1 kcal·mol^{-1}. This stability of the $-60°$ form for χ-6′ can be attributed to the H-bond between O-6′ and O-6 while O-6″ participates in no intramolecular H-bond (Fig. 4).

Our results indicate that at least two staggered from each of the χ-6 pendant groups should be present in significant amounts. Our spectral analysis supports this proposal. The protons on C-6, C-6′, and C-6″ are all diastereotopic, but each pair shows only one signal, suggesting equilibration of different staggered forms resulting in nearly equal deshielding for both protons. Given the small energy differences among the various conformations, it is not surprising that the forms found in the crystal were not the same as the lowest energy forms found in this work. Intermolecular H-bonding will certainly be able to affect rotation of these flexible groups.

On the other hand, χ-1″ clearly prefers one of the staggered forms, $+60°$. The n.m.r. results show splitting between the protons on C-1″, but unfortunately the splitting is not sufficient to allow for selective observation of each proton. As a result we could gain no experimental information on the orientation of this side group.

Inspection of Table II shows that there are numerous structures populated with different side group positions. So, while there appears to be one populated linkage form, the side groups have many different rotamers populated.

We would have preferred to treat all torsion angles, φ, ψ, φ', ψ', ω, χ-6, χ-6', χ-6'', and χ-1 as independent variables, but even looking only at the staggered forms this would have meant 3^8 or 6561 structures to minimize. While it is possible that a low-energy structure was missed by not carrying out a full, independent analysis, this appears unlikely because the pendant groups appear to make a minor contribution to the total steric energy and can thus justifiably be treated as a secondary factor.

Ring conformations. — Table III described the forms of the rings in the starting structures and in the lowest energy structures. The greatest variations in ring conformation during the surveys were found when the combinations of the driven torsion angles caused severe steric conflicts between rings. Still, the glucopyranose ring was quite inflexible, but the fructofuranose ring had substantial flexibility. The favored conformation of the glucopyranose ring agreed with that from molecular dynamics[16], $^4C_1$, and the fructofuranose rings were generally similar to those found earlier to be preferred for the monosaccharide[13], ^4_3T.

Fig. 3 illustrates, on a Cremer–Pople wheel, the ranges of the fructofuranose ring conformations that occurred during our surveys of linkage conformations. Furanose ring 1 suffered greater distortion, perhaps because C-2' of fructose 1 is linked to both other rings. However, the "southern" ^3_4T ($\varphi_2 = 90°$) conformation found in crystalline **1** was not induced at any of the tested conformations. When the crystal structure was fully optimized (XR3), the ring changed to the ^5_4T form ($\varphi_2 = 119°$), but not to a "northen" conformation, confirming that the northern/southern barrier[13] exists here, too. A majority of the structures and all the low-energy structures observed had ^4_3T or adjacent forms, the same as the predicted minimum for the monomer ($\varphi_2 = 262°$) (ref. 13).

The range of φ_2 values found for fructose 2 was nearly as wide, but more than 90% of the values fell within the narrower range of $\varphi_2 = 243°$–$296°$, and most of the output structures had a ^4_3T or $_3E$ conformation. The crystallographic conformation, $_3E$ ($\varphi_2 = 245°$), of fructose 2 in **1** is similar to the low-energy forms found in the calculations. The global minimum again had a fructose 2 conformation of ^4_3T ($\varphi_2 = 272°$).

Vicinal coupling constants are dependent on torsion angles[17], and the H-3–H-4 and H-4–H-5 fructofuranose couplings are very sensitive to ring puckering. The similarities between the $^3J_{H-H}$ of H-3'–H-4' and of H-3''–H-4'' (Table IV) point to the same conformation of the fructose 1 and fructose 2 rings in solution, namely the ^4_3T form. It is possible that other conformations may be present in small amounts, but due to the difference in coupling constants, it is unlikely that fructose 1 exists as the southern conformer in any significant amount.

The glucose ring is less flexible than the fructose ring, and, as shown by molecular dynamics simulations carried out on the glucose ring[16], the glucose ring tends to favor the $^4C_1$ conformation. Results from all the searches carried in this work also shows that the glucose ring retains its $^4C_1$ conformation, varying only when there are severe steric interactions. The $^3J_{C-H}$ observed between H-1 and C-3 and between H-1 and C-5 in the

selective *J*-resolved spectrum confirmed that the glucose ring has the $^4C_1$ conformation in solution. The observed coupling constants, $^3J_{H\text{-}1\text{-}C\text{-}3} = 6.3$ Hz and $^3J_{H\text{-}1\text{-}C\text{-}5} = 6.1$ Hz, could only be possible if the glucose ring assumes the $^4C_1$ conformation.

CONCLUSIONS

The flexibility of the furanose ring is a modeling challenge, because it introduces additional degrees of freedom, and even in trimers that contain a furanose, it is unreasonable to address all conformational space. So, in order to understand the structures of inulin and the inulin-type oligomers, we previously studied the conformations of the principal monomer and dimer groups, fructofuranose and inulobiose, and applied the results here.

Unfortunately, neither the monomer nor the dimer fructofuranose model was suited to much experimental confirmation, since they are reducing sugars, and the reducing fructose residue would be found principally in the pyranose form. In the present work on 1-kestose, we have been able to compare the model with experimental data from n.m.r. spectroscopy and literature single-crystal X-ray diffraction[9].

A notable result of this study is that molecular modeling predicts a form of **1** which was also observed by n.m.r. spectroscopy taken in D_2O solution, but the flexibility of the furanose ring apparently results in the distortion of one ring when crystallization occurs. This result is a reminder that crystalline conformations, particularly in flexible hydrogen-bonding compounds, can be different from their solution form.

ACKNOWLEDGMENTS

We would like to thank John W. Tesch of the IBM Dallas National Engineering and Scientific Support Center and Jeffrey B. Sipior for help with implementing the MM2(87) program on the IBM 3081.

REFERENCES

1 N. Albon, D. J. Bell, P. H. Blanchard, D. Gross, and J. T. Rundell, *J. Chem. Soc.*, (1953) 24–27.
2 I. R. Siddiqui and B. Furgala, *J. Apicult. Res.*, 7 (1968) 51–59.
3 G. Hendry, *New Phytol.*, 106 (1987) 201–216.
4 H. G. Pontis, *J. Plant Physiol.*, 134 (1989) 148–150.
5 A. Fuchs, *Starch/Stärke*, 39 (1987) 335–374.
6 V. Tran and J. W. Brady, *Biopolymers*, 29 (1990) 961–979.
7 T. M. Calub, A. L. Waterhouse, and A. D. French, *Carbohydr. Res.*, 207 (1990) 221–235.
8 T. M. Calub, A. L. Waterhouse, and N. J. Chatterton, *Carbohydr. Res.*, 199 (1990) 11–17.
9 G. A. Jeffrey and Y. J. Park, *Acta Crystallogr. Sect. B*, 28 (1972) 257–267.
10 N. L. Allinger, *J. Am. Chem. Soc.*, 99 (1977) 8127–8134.
11 A. D. French, V. Tran, and S. Perez, in A. D. French and J. W. Brady (Eds.), *Computer Modeling of Carbohydrate Molecules*; ACS Symp. Ser. 430; American Chemical Society, Washington, DC, 1990, pp. 191–212.
12 L. Nørskov-Lauritsen and N. L. Allinger, *J. Comput. Chem.*, 5 (1984) 326–335.
13 A. D. French and V. Tran, *Biopolymers*, 29 (1990) 1599–1611.
14 I. Tvaroška, M. Hricovíni, E. Petráková, *Carbohydr. Res.*, 189 (1989) 359–62.

15 M. Hricovini, I. Tvaroška, J. Hirsch, *Carbohydr. Res.*, 198 (1990) 193–203.
16 J. W. Brady, *J. Am. Chem. Soc.*, 108 (1986) 8153–8160.
17 C. A. G. Haasnoot, F. A. A. M. DeLeeuw, and C. Altona, *Tetrahedron*, 36 (1981) 2783–2792.